

Cross-Domain Generalization: Enhancing Rare Disease Data Representation using Diffusion

Wonseok Oh

University of Michigan
Electrical Engineering and Computer Science

Abstract. We introduce a Schrödinger Bridge method to generate datasets from diverse domains. This enables the collection of data for rare diseases and limited datasets. Therefore, in this paper, we introduce **Domain Knowledge Diffusion Model (DKDM)** using Schrödinger Bridge to generate rare disease images and limited data in medical imbalance datasets. Our method demonstrates the capability to generate cross-domain generalized images for rare diseases beyond utilizing a single-domain dataset by training the separated model with domain datasets. Also, our method surpasses the existing Schrödinger Bridge diffusion models by using domain phase loss. Furthermore, we show that utilizing images generated from our method is more competitive than training with existing methods.

Keywords: Cross-Domain Generation · Diffusion models · Data Augmentation

1 Introduction

Deep learning has achieved remarkable progress in computer-aided diagnosis.[15, 27, 17, 14] Recently, numerous studies utilizing diffusion methods have demonstrated successive success. There are two main ways to use diffusion methods in medical imaging. Firstly, anomaly detection utilizes methods that combine deterministic iterative noising and denoising schemes.[24, 1, 29] Secondly, by using rare disease data, the diffusion model generates images of these domain.[12, 5]. However, these methods show significant performance yet rely on training with large datasets. Many attempts have been made to train the generative model with limited data[24, 5, 13], but it still requires large datasets or only single domain datasets. By utilizing limited data or multi-domain datasets, training a generative model with good quality and high fidelity seems limited. Domain adaption and cross-domain generalization approaches show their generalization ability across diverse datasets.[25, 4, 9] Specifically, domain adaption is a commonly used technique that fine-tunes generators and discriminators on target datasets. These are usually based on the generative models. In particular, after training the model with the source domain, a few parameters are fine-tuned, and regularization methods are added to transfer knowledge about the target

domain.[24, 5] However, resulting diversity is typically less semantic and produces only very similar images. Therefore, more advanced methods are required for good quality and high fidelity. For this reason, we conducted training models with various domain datasets using the Schrödinger Bridge. This is used to generate cross-domain generalized images to balance datasets for imbalanced datasets. Here, we find that transferring the trained model with the source domain directly to target-domain knowledge results in a loss of prior knowledge. To address problems, we utilize domain phase loss to minimize the cosine similarity of the reconstructed image and target domain. Since similar phases are observed in datasets in the same domain, the method of reducing loss in the domain transfer process is meaningful in creating cross-domain data. Also, we explore why diversity drops when utilizing diversity datasets and how to produce highly diverse images in multi-domain datasets. To that end, we introduce **Domain Knowledge Diffusion Models(DKDM)** using cross-domain generalization technique to generate rare disease images with limited data in medical imbalance datasets. The idea behind **DKDM** is to learn various domain representations. Compared to the conventional strategy, since utilizing design loss for domain generalization, **DKDM** can produce high-fidelity images without catastrophic forgetting problems for source domain datasets. Specifically, we demonstrate that **DKDM** is competitive for generating images compared to existing methods. Also, When the training model utilizes the existing dataset with generated images, we show competitive performance. Through extensive experiments, our contributions follow that:

- Our methods demonstrate the capability to generate cross-domain generalized images for rare diseases beyond utilizing a single-domain dataset by training the model with multiple diverse domain datasets.
- Domain phase loss resolves the issue of losing prior knowledge when directly transferring a trained model from the source domain to the target domain.
- We show competitive performance among the existing unpaired image-to-image translation models.

2 Methods

2.1 Schrödinger Bridge (SB)

A Schrodinger bridge extension of score-based generative models (SGMs) has been introduced to transfer from an initial distribution to a terminal distribution over time. It is closely related to probability theory and stochastic control. To approximate score-based generative models (SGMs), [3, 22] introduce leveraging Iterative Proportional Fitting (IPF) algorithm and [18, 8] introduced similar algorithms. With the successive success of research utilizing SB, several variants have come on to the diverse stage, such as Probabilistic Lambert Problem, inverse problems[16], Mean-Field Games[10], constrained transport problems[20], Riemannian manifolds[21], and path samplers[28, 26]. [23] investigate entropy interpolation between Dirac delta and noisy data with SB in the unsupervised setting. Otherwise, in the supervised setting, I2SB[11] and InDI[7] used paired data

to learn SBs between Dirac delta and data while finding the continuous path. Recently, DDIB[19] tried to not unpaired data but concentrate two SBs between different domain pairs data and demonstrated utility in a wide variety of translation tasks. However, to the best of our knowledge in the Medical community, the SB problem has not been investigated between Unpaired image-to-image translation. Thus, our work endeavors to demonstrate that inherent optimal transport properties are achievable in various aspects by utilizing paired or unpaired images. Also, our work tried to adapt various datasets to demonstrate scalability. Our model is based on an elaborate Schrödinger Bridge, which elucidates that SB can be articulated as a sequential integration of generators determined via adversarial learning paradigms. More precisely, considering a partition $\{t_i\}_{i=0}^N$ of the unit interval $[0, 1]$ with and $t_0 = 0$, $t_N = 1$, and $\tilde{x}_0 = x_{t_0}$, $\tilde{x}_N = x_{t_N}$, we can represent sb via the Markov chain decomposition.

$$p(\{\tilde{x}_n\}) = p(\tilde{x}_N|\tilde{x}_{N-1})p(\tilde{x}_{N-1}|\tilde{x}_{N-2}) \cdots p(\tilde{x}_1|\tilde{x}_0)p(\tilde{x}_0) \quad (1)$$

Through decomposition , we learn $p(\tilde{x}_{i+1}|\tilde{x}_i)$ presuming we can sample from $p(\tilde{x}_i)$ (for $i = 0, \dots, N - 1$). Thus, we can learn $p(\tilde{x}_{i+k}|\tilde{x}_{i+(k+1)})$ and so forth. Consider $q_{\phi_i}(\tilde{x}_1|\tilde{x}_i)$, a conditional distribution orchestrated by a DNN with parameters ϕ_i . This is also the denoising and generation step, which estimates the target domain image x_i . Therefore, we optimize ϕ_i with the arbitrary step i .

2.2 Model operations of DKDM

Model Description Our model embarks on optimizing a loss function for a randomly selected time step t_i during the training stage. The inception of the model involves sampling an image x_{t_i} from the initial domain and a corresponding image from the target distribution denoted by x_1 . The target distribution is signified by π_1 , and the details of the sampling procedure for x_t will be elucidated shortly.

The sampled image x_t is subsequently processed through a transformation function $q_{\phi}(x_1|x_t)$, yielding $x_1(x_t)$, which is an estimation of the target domain data given x_t . The pairs $(x_t, x_1(x_t))$ and $(x_1, x_1(x_t))$ are utilized to compute the $\mathcal{L}_{SB}(\phi, t_i)$ and the Adversarial Loss $\mathcal{L}_{Adv}(\phi, t_i)$. Here, $\mathcal{L}_{SB}(\phi, t_i)$ measures the discrepancy between the learned distribution q_{ϕ} and the true data distribution in the context of a time step t_i in a Markov chain. Specifically, the \mathcal{L}_{SB} is defined as an expectation over the data distribution of the squared Euclidean distance between x_{t_i} and $x_{t_{i+1}}$, regularized by a term involving the entropy of the learned distribution q_{ϕ} . The entropy component in \mathcal{L}_{SB} is estimated through a mutual information estimator, leveraging the relationship $I(X, X) = H(X)$ for a random variable X , where I represents mutual information. The divergence in \mathcal{L}_{Adv} is evaluated utilizing adversarial learning techniques, with x_1 and $x_1(x_t)$ serving as the "real" and "fake" inputs to the discriminator.

Sampling Procedure The intermediate and final samples are generated through a procedure that simulates a Markov chain, as described above, using the transformation function q_{ϕ} . Commencing with x_t , we predict the image in the

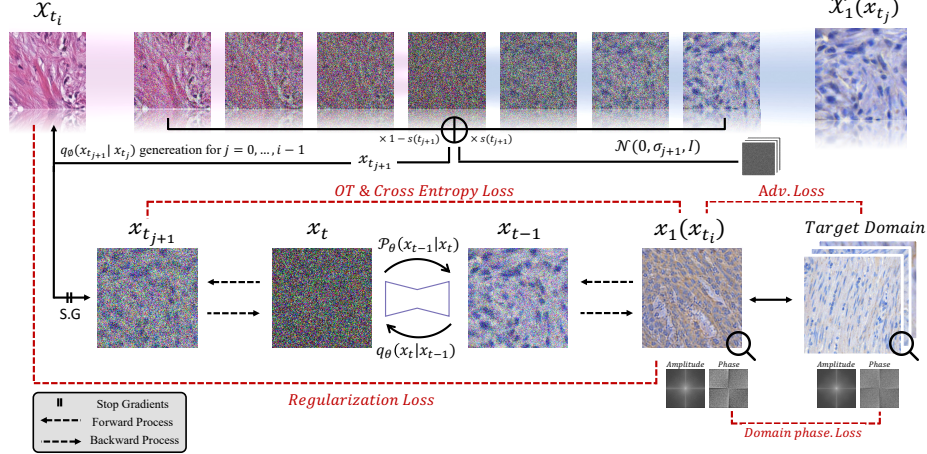


Fig. 1. The process begins with an initial set of sample images x_{t_i} . These images are subjected to a series of transformations involving the addition of noise through a process defined by the function q_ϕ . As the images pass through each step, they become increasingly noisy, simulating a Markov chain. The images are then processed through a stochastic gradient (S.G) operation and a backward process that aims to recover the original image features from the noise, indicated by the function $p_\theta(x_{t-1}|x_t)$. Throughout this transformation process, several loss functions are employed.

target domain $x_1(x_t)$ through iterative sampling and the application of Gaussian noise, facilitating the generation of $x_{t_{j+1}}$. This iterative procedure enhances the prediction of the target domain sample, thereby refining it through the trajectory $\{x_1(x_t) : i = 0, \dots, N - 1\}$.

Process Illustration Figure 1 encapsulates the generation stage of the model, elucidating the transformation from the original domain X_{t_i} to the target domain $X_1(x_{t_j})$. The illustration conveys the integration of various machine learning paradigms, including stochastic processes, adversarial training, regularization, and potentially Fourier analysis, to effectuate this domain transformation.

2.3 Resolving Prior Knowledge Loss

If datasets with a very large difference between domains are generalized, plenty of existing information on images is lost when translating input data from the source domain to the target domain. This phenomenon occurs when new images are filled only with information from other domains while information is put in a specific domain. Our goal was to solve this problem. Since medical data have biases for each data, there is a big difference between domains. We used the Fourier transform for each dataset to show amplitude and phase. As a result, as can be seen in the 2, it was confirmed that data belonging to the same domain have similar amplitude and phase, and in the case of data in different domains,

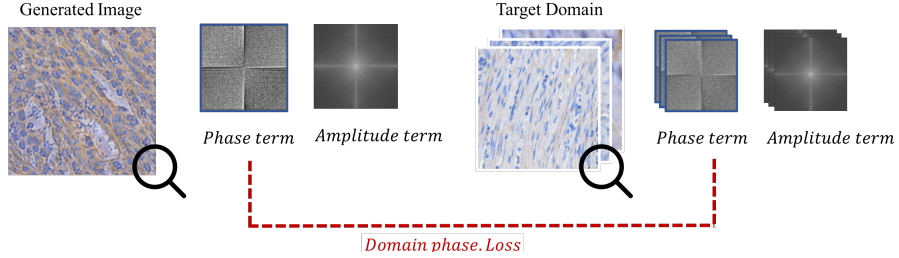


Fig. 2. We employ Fourier transformation on both the generated and target domain images to analyze texture. The loss function applied to the model utilizes cosine similarity in the Phase term, representing the texture. However, the Amplitude term is not utilized.

the difference was found to be very large. Based on this, we designed a domain phase loss function for optimization.

$$\mathcal{L}_{\mathcal{DP}} = \frac{\sum_{i,j} \text{Phase } (\mathcal{X})_{i,j} \cdot \text{Avg}(\hat{X})_{i,j}}{\sqrt{\sum_{i,j} (\text{Phase } (\mathcal{X})_{i,j})^2} \cdot \sqrt{\sum_{i,j} (\text{Avg}(\hat{X})_{i,j})^2}} \quad (2)$$

where \mathcal{X} means generated image and \hat{X} means Average for getting phase term numerical value from target domains. In short, the domain phase loss function measures the cosine similarity of the phase of the generated image and the phase of the average target domain.

We also add regularization loss to make the final objective for **DKDM**. To further refine the **DKDM** objective, regularization is introduced to compel the generator network q_ϕ to uphold a consistency between the predicted outcome x_1 and the initial state x_0 :

$$\mathcal{L}_{\text{Reg}}(\phi, t_i) = E_{p(x_0, x_t)} E_{q_\phi(x_1|x_t)} [S(x_0, x_1)] \quad (3)$$

In this context, S denotes a scalar, differentiable function that encapsulates a domain-specific measure of resemblance between its two inputs. Essentially, S encodes our preconceived notion of similarity across image pairs. We can derive the final loss function here by incorporating the previously introduced Adversarial Loss and Schrödinger Bridge Loss term. Consequently, the amended **DKDM** objective at time t_i can be stated as:

$$\mathcal{L}_{\text{DKDM}}(\phi, t_i) = \mathcal{L}_{\text{Adv}}(\phi, t_i) + \lambda_{\mathcal{DP}, t_i} \mathcal{L}_{\mathcal{DP}}(\phi, t_i) + \lambda_{\mathcal{SB}, t_i} \mathcal{L}_{\mathcal{SB}}(\phi, t_i) + \lambda_{\text{Reg}, t_i} \mathcal{L}_{\text{Reg}}(\phi, t_i) \quad (4)$$

This is the definitive goal within our **DKDM** scheme.

3 Experiments and Results

3.1 Implementation details

Our proposed methods use Markovian discriminator in \mathcal{L}_{Adv} and utilize patch-wise contrastive matching in \mathcal{L}_{Reg} . For training DKDM network for 10 epochs with batch size 1 and Adam optimizer with $\mathcal{B}_1 = 0.5$, $\mathcal{B}_2 = 0.9999$,. We also set $\lambda = 0.0002$ for the initial learning rate, learning decay 500, and $\mathcal{L}_{dp} = 0.1$ for Domain phase loss. We resized the input image 256×256 and normalized it into the range $[-1, 1]$. For SB training and simulation, we divided the unit interval $[0, 1]$ into 5 uniform space intervals with uniform spacing. We adopt entropy estimation [2] to our model. We apply the data augmentation method following previous work. However, unlike previous studies, we applied the mentioned settings consistently to both the Epithelium-Stroma and ISIC2019 datasets. We used the PyTorch library with single V100 GPU to train Epithelium-Stroma and ISIC2019 datasets, which took around 3 and 5 hours.

3.2 Qualitative Analysis

To substantiate the continual improvement of our proposed methodology in achieving a seamless transformation of texture to the target domain, avoiding over-fitting compared to conventional methods, we have undertaken the visualization of consecutively transformed images. This visualization serves as evidence for the ongoing enhancement and stability of our approach as the texture progressively evolves into the target domain without succumbing to overfitting issues. 3 illustrates the transformation results between the NCH and IHC datasets, and vice versa, from IHC to NCH. Similarly, the transformations between Melanocytic and Carcinoma datasets and the reverse from Carcinoma to Melanocytic are depicted. The degree of Style Guidance indicates the number of iterations our model has undergone to produce the outcomes; the images on the far left contain the most information from the original data, progressing towards the right; they increasingly resemble the target domain. Notably, during the testing phase, the images resembling the target domain were generated without any target domain information, based solely on randomly sampled images from the source domain.

3.3 Quantitative Analysis

To assess quantitative metrics, we compared the Fréchet Inception Distance (FID) [6] scores with those of existing methods.1 The evaluation focused on the FID scores during the conversion process from NCH to IHC and vice versa. Given the nature of the FID score, which compares the images themselves, we observed that the scores were relatively high, which is attributable to our dataset's characteristic of being comprised of unpaired images across different domains. Upon comparison, it was evident that our model achieved lower FID scores than the pre-existing UNSB model. This trend of reduced FID scores was consistent even

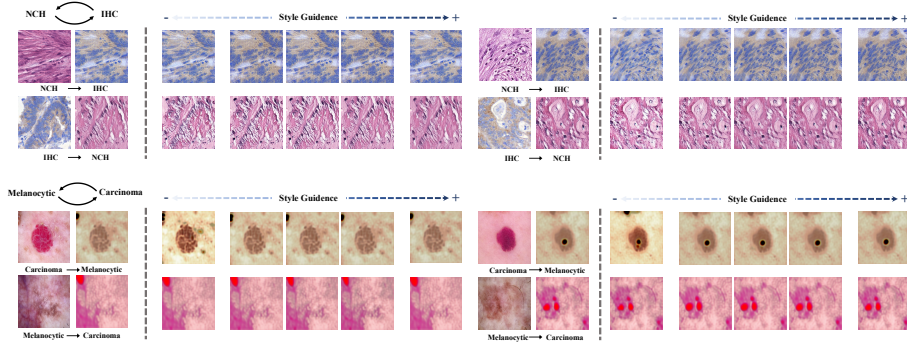


Fig. 3. For qualitative evaluation of image-to-image translation results from our DKDM, we transfer input images into different medical domain images and style images. We also show successively refining the predicted target domain image.

when the domain conversion was reversed in our experiments. These findings corroborate the efficacy of our domain phase loss in mitigating the disparities between domains, thereby validating its role in bridging the domain gap. Additionally, as depicted in Figure 5, it is observed that our model converges after approximately 100 iterations of the training steps. This applies to both scenarios: transforming fake images into target images and converting fake images into real images.

Model	NCH→IHC ↓	IHC→ NCH ↓
UNSB	365.38	157.16
DKDM(Ours)	307.52	102.08

Table 1. The quantitative FID score for the reconstructed images. Our model surpasses the FID score of the state-of-the-art model UNSB

3.4 Gray-scale image to image translation

Recently, few studies have proposed diffusion models for image transfer using gray-scale images. Therefore, we applied our proposed method to explore the efficacy of gray-scale image to image transfer, specifically on CheXpert images, aiming to assess its performance across unpaired images. However, Gray-scale image transfer is limited due to the absence of color information. It is also typically composed of fine-grained disease. The experiments are shown in Fig 4.

3.5 Detailed imagery description of DKDM

DKDM can generate images that align with the target domain while preserving certain aspects of the source domain. As depicted in Fig 5, **DKDM**, unlike the state-of-the-art model UNSB, adeptly retains features of the source domain's

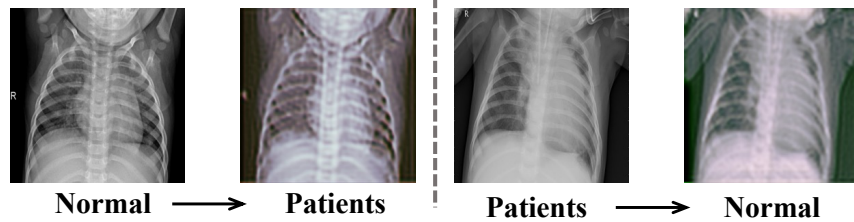


Fig. 4. To demonstrate our proposed method well on the gray-scale image translation task, we utilize the CheXpert dataset. In particular, we tried to transfer images from patient data to normal data.

images while accurately producing images suitable for the target domain. This can be attributed to the domain phase loss, which effectively minimizes the differences between the domains. In the case of UNSB, it is noted that as the number of evaluations increases, the distinctive features of the original source domain gradually diminish. In contrast, our model maintains the characteristics of the source domain well while approaching the target domain.

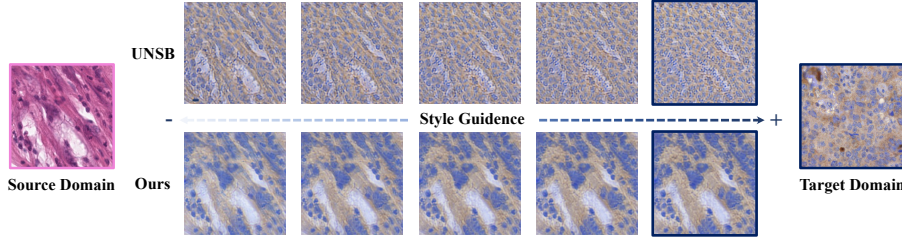


Fig. 5. DKDM can be possible to iteratively enhance the anticipated image of the target domain, allowing the model to adjust intricate elements while maintaining the texture.

4 Conclusions

We introduce **DKDM**, which enhances UNSB utilizing Schrödinger Bridge(SB) and combines SB with GAN training techniques for unpaired image-to-image translation by adding Domain phase term loss. We demonstrated the efficacy and prospects of **DKDM** by extensive experiments on the unpair domain data or Different classes from the same dataset. Unlike existing models, we have confirmed that **DKDM** preserves the appearances from the source domain well while generating images suitable for the target domain. We also highlight the significance and limitations of the gray-scale image transfer task, identifying it as a challenge that needs to be addressed in future research endeavors.

References

1. Behrendt, F., Bhattacharya, D., Krüger, J., Opfer, R., Schlaefer, A.: Patched diffusion models for unsupervised anomaly detection in brain mri. arXiv preprint arXiv:2303.03758 (2023)
2. Belghazi, M.I., Baratin, A., Rajeswar, S., Ozair, S., Bengio, Y., Courville, A., Hjelm, R.D.: Mine: mutual information neural estimation. arXiv preprint arXiv:1801.04062 (2018)
3. De Bortoli, V., Thornton, J., Heng, J., Doucet, A.: Diffusion schrödinger bridge with applications to score-based generative modeling. Advances in Neural Information Processing Systems **34**, 17695–17709 (2021)
4. Dong, J., Cong, Y., Sun, G., Zhong, B., Xu, X.: What can be transferred: Unsupervised domain adaptation for endoscopic lesions segmentation. In: Proceedings of the IEEE/CVF conference on computer vision and pattern recognition. pp. 4023–4032 (2020)
5. Gong, K., Johnson, K., El Fakhri, G., Li, Q., Pan, T.: Pet image denoising based on denoising diffusion probabilistic model. European Journal of Nuclear Medicine and Molecular Imaging pp. 1–11 (2023)
6. Heusel, M., Ramsauer, H., Unterthiner, T., Nessler, B., Hochreiter, S.: Gans trained by a two time-scale update rule converge to a local nash equilibrium. Advances in neural information processing systems **30** (2017)
7. Kawar, B., Elad, M., Ermon, S., Song, J.: Denoising diffusion restoration models. Advances in Neural Information Processing Systems **35**, 23593–23606 (2022)
8. Léonard, C.: Some properties of path measures. Séminaire de Probabilités XLVI pp. 207–230 (2014)
9. Li, D., Yang, J., Kreis, K., Torralba, A., Fidler, S.: Semantic segmentation with generative models: Semi-supervised learning and strong out-of-domain generalization. In: Proceedings of the IEEE/CVF Conference on Computer Vision and Pattern Recognition. pp. 8300–8311 (2021)
10. Liu, G.H., Chen, T., So, O., Theodorou, E.: Deep generalized schrödinger bridge. Advances in Neural Information Processing Systems **35**, 9374–9388 (2022)
11. Liu, G.H., Vahdat, A., Huang, D.A., Theodorou, E.A., Nie, W., Anandkumar, A.: I Θ sb: Image-to-image schr\"{o}dinger bridge. arXiv preprint arXiv:2302.05872 (2023)
12. Mao, Y., Jiang, L., Chen, X., Li, C.: Disc-diff: Disentangled conditional diffusion model for multi-contrast mri super-resolution. arXiv preprint arXiv:2303.13933 (2023)
13. Ruiz, N., Li, Y., Jampani, V., Pritch, Y., Rubinstein, M., Aberman, K.: Dream-booth: Fine tuning text-to-image diffusion models for subject-driven generation. In: Proceedings of the IEEE/CVF Conference on Computer Vision and Pattern Recognition. pp. 22500–22510 (2023)
14. Shen, L., Yu, L., Zhao, W., Pauly, J., Xing, L.: Novel-view x-ray projection synthesis through geometry-integrated deep learning. Medical image analysis **77**, 102372 (2022)
15. Shen, L., Zhu, W., Wang, X., Xing, L., Pauly, J.M., Turkbey, B., Harmon, S.A., Sanford, T.H., Mehralivand, S., Choyke, P.L., et al.: Multi-domain image completion for random missing input data. IEEE transactions on medical imaging **40**(4), 1113–1122 (2020)
16. Shi, Y., De Bortoli, V., Deligiannidis, G., Doucet, A.: Conditional simulation using diffusion schrödinger bridges. In: Uncertainty in Artificial Intelligence. pp. 1792–1802. PMLR (2022)

17. Song, Y., Shen, L., Xing, L., Ermon, S.: Solving inverse problems in medical imaging with score-based generative models. arXiv preprint arXiv:2111.08005 (2021)
18. Song, Y., Sohl-Dickstein, J., Kingma, D.P., Kumar, A., Ermon, S., Poole, B.: Score-based generative modeling through stochastic differential equations. arXiv preprint arXiv:2011.13456 (2020)
19. Su, X., Song, J., Meng, C., Ermon, S.: Dual diffusion implicit bridges for image-to-image translation. arXiv preprint arXiv:2203.08382 (2022)
20. Tamir, E., Trapp, M., Solin, A.: Transport with support: Data-conditional diffusion bridges. arXiv preprint arXiv:2301.13636 (2023)
21. Thornton, J., Hutchinson, M., Mathieu, E., De Bortoli, V., Teh, Y.W., Doucet, A.: Riemannian diffusion schrödinger bridge. arXiv preprint arXiv:2207.03024 (2022)
22. Vargas, F., Thodoroff, P., Lamacraft, A., Lawrence, N.: Solving schrödinger bridges via maximum likelihood. Entropy **23**(9), 1134 (2021)
23. Wang, G., Jiao, Y., Xu, Q., Wang, Y., Yang, C.: Deep generative learning via schrödinger bridge. In: International Conference on Machine Learning. pp. 10794–10804. PMLR (2021)
24. Wolleb, J., Bieder, F., Sandkühler, R., Cattin, P.C.: Diffusion models for medical anomaly detection. In: International Conference on Medical image computing and computer-assisted intervention. pp. 35–45. Springer (2022)
25. Xu, X., Chen, Y., Wu, J., Lu, J., Ye, Y., Huang, Y., Dou, X., Li, K., Wang, G., Zhang, S., et al.: A novel one-to-multiple unsupervised domain adaptation framework for abdominal organ segmentation. Medical Image Analysis **88**, 102873 (2023)
26. Zhang, Q., Chen, Y.: Path integral sampler: a stochastic control approach for sampling. arXiv preprint arXiv:2111.15141 (2021)
27. Zhang, Z., Jiang, R.: User-centric democratization towards social value aligned medical ai services. In: Proceedings of the Thirty-Second International Joint Conference on Artificial Intelligence. pp. 6326–6334 (2023)
28. Zheng, C., Cham, T.J., Cai, J.: The spatially-correlative loss for various image translation tasks. In: Proceedings of the IEEE/CVF conference on computer vision and pattern recognition. pp. 16407–16417 (2021)
29. Zhou, D., Yang, Z., Yang, Y.: Pyramid diffusion models for low-light image enhancement. arXiv preprint arXiv:2305.10028 (2023)

1 Detail of datasets

We evaluate the proposed method with multiple Epithelium-Stroma, CheXpert, and ISIC2019 datasets. Epithelium-Stroma datasets(e.g IHC and NCH) are common publicly available datasets. The datasets were collected from different methods and institutions, which caused the domain shift among them, and they were labeled as epithelium or stroma. The IHC datasets contain 10015 histopathological images, and NCH datasets contain a total of 8015 images. We generate stylized images of the epithelium class in the IHC dataset within the NCH dataset, corresponding to the same class. We also apply the reverse scenario. The CheXpert dataset compose of 14 classes with 224,319 images. Due to limitations in incorporating all available data into the training, we opted to sample the image for experimentation purposes. The ISIC2019 dataset has 8 classes with 25,331 images and can be found publicly. For qualitative comparison, we also utilize the ISIC2019 dataset to demonstrate the leverage for transfer among images of different classes within pairs that belong to the same domain.

Datasets	class	samples	imbalance ratio	domain
IHC	2	820	1.5	•
NCH	2	24,763	1.3	•
ISIC2019	8	25,331	53.8	
CheXpert	14	224,316	37.9	

Table 1. The details of medical datasets. We utilized IHC and NCH for the unpaired image-to-image transfer task, while applying class-wise transfer to CheXpert and ISIC2019.

2 Qualitative result of losses

The graph of the quantitative analysis of the loss metrics during the training phase indicates a notable trend towards convergence, achieved at the threshold of approximately 100 iterations. This observation suggests that the model begins to reach a stable state where further iterations result in diminishing improvements to loss reduction. Convergence in this context implies that the model has effectively assimilated the underlying patterns within the training dataset to a degree where it can now yield consistent predictions or outputs.

3 Limitations

Despite generating a generalized image and showing competitive performance, our proposed **DKDM** still has limitations in terms of twofold. Firstly, we could use diffusion pre-trained by large datasets. A pre-training model with large

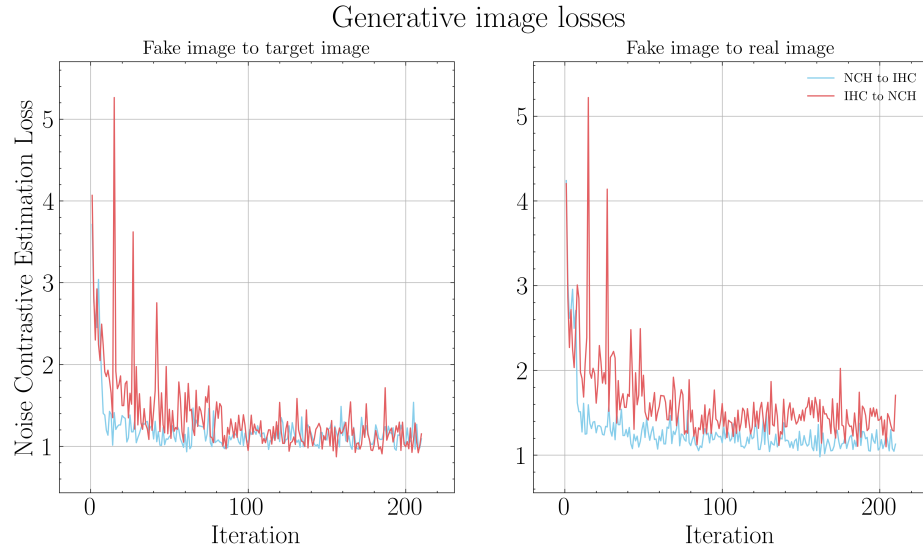


Fig. 1. Quantitative graph of the losses while training the models. This shows the model almost converges from 100 iterations.

datasets is highly unlikely to cause catastrophic forgetting compared to not. Secondly, in datasets comprising fine-grained medical images (such as epithelium-stroma and ISIC2019, etc..), the image-to-image transfer did not clearly demonstrate the generation of distinct images. This issue arises due to variations in individual genetic characteristics, even for the same medical condition. Additionally, our experiments aim to generate generalized images. For these reasons, It is not sure that it will work well on other tasks(Classification, Detection, Segmentation, etc.). Specifically, since the generated image and existing datasets are different in terms of density, it is not certain whether they will improve density prediction. (e.g. segmentation). Also, when we adapt to gray-scale image datasets, transferring texture isn't impossible. Thus, we believe that developing a diffusion model with universal applicability across both unpaired gray-scale and RGB domains would be an intriguing avenue for future research.